EFFECT OF ANTENNA SIZE ON ROCK MASS BREAKING EFFICIENCY UNDER OPEN-ENDED MICROWAVE TREATMENT

by

Shou-Ning XUE[a,b], Yang ZHANG[b*], Jun LUO[c], Fei-Long XU[c], and Ben-Gao YANG[b]

[a] State Key Laboratory of Intelligent Construction and Healthy Operation and Maintenance of Deep Underground Engineering, College of Civil and Transportation Engineering, Shenzhen University, Shenzhen, Guangdong, China
[b] State Key Laboratory of Intelligent Construction and Healthy Operation and Maintenance of Deep Underground Engineering, College of Water Resource and Hydropower, Sichuan University, Chengdu, Sichuan, China
[c] China Construction Third Bureau First Engineering Co., Ltd., Wuhan, China

Original scientific paper
https://doi.org/10.2298/TSCI2502259X

Antenna size is a critical factor influencing the efficiency of open-ended microwave rock-breaking. An electromagnetic-thermal-mechanical coupling model was developed to systematically investigate the influence of antenna size on the temperature distribution within the rock mass under microwave treatment. Furthermore, the evolution of rock mass damage was analyzed based on the stress filed induced by microwave treatment. The results demonstrate that decreasing the antenna size can significantly enhance the electromagnetic power loss density, thereby accelerating the rock-breaking process. However, a moderate increase in antenna size can broaden the extent of rock mass damage and improve the overall efficiency of microwave energy utilization.

Key words: *rock breaking, microwave, numerical model*

Introduction

Microwave rock breaking has the advantages of low disturbance and environmentally friendly, with promising prospects for engineering applications [1-3]. However, current research on the heating and fracture mechanisms of rock under microwave treatment remains largely confined to small-scale samples, with the majority of experimental studies conducted within microwave resonant cavities. Therefore, the existing research is insufficient to support the further application of microwave rock-breaking technology, it is essential to conduct targeted research that is closely aligned with practical application scenarios. Feng *et al*. [4] conducted field test of high power microwave-assisted mechanical excavation study the influence of antenna type and working distance on the heating properties of rock masses under microwave treatment. Ma *et al.* [5] evaluated the rock-breaking performance of various waveguide types and analyzed the effect of rock size on the efficiency of open-ended microwave rock breaking. Additionally, Gao *et al*. [6] explored the potential applications of open-ended microwave rock breaking technology in drilling.

* Corresponding author, e-mail: zy0501a@163.com

Based on the previous research, this study develops an electromagnetic-thermal-mechanical coupling model to investigates the effect of antenna size on the temperature characteristics and damage evolution process of rock masses under microwave treatment.

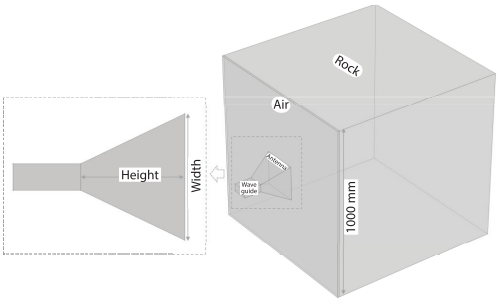

Figure 1. Geometry model diagram

Table 1. parameters of numerical model

Parameter	Value
Heat capacity [$Jkg^{-1}K^{-1}$]	1050
Heat conductivity [$Wm^{-1}K^{-1}$]	1.85
Relative permittivity	4.87-0.332*J
Density [kgm^{-3}]	2700
Compressive strength [MPa]	UCS(T)
Tensile strength [MPa]	0.1*UCS(T)
Elastic modulus [GPa]	20.28
Poisson's ratio	0.2
Internal friction angle [rad]	$\pi/4$

Model construction

Geometry model and parameter settings

The model constructed in this study consists of rock mass, air, BJ26 rectangular waveguide operating at 2.45 GHz in TE_{10} mode, and a horn antenna with a square port. As shown in fig. 1, the rock mass is set up as a cube with a side length of 1000 mm, and the thickness of the air layer between the antenna and the rock mass is 10 mm. The material properties of the waveguide and antenna are defined as copper and their electromagnetic field boundary conditions are set to impedance boundary conditions. During the simulation process, only the heating process of the rock mass is considered, while microwave loss during air propagation is ignored. The electromagnetic field boundary condition for the rock mass and the air is defined as a scattering boundary condition, and the convective heat transfer coefficient at the rock mass boundary is set to 20 W/m^2K, the initial temperature of the rock mass was set at 298.15 K. The physical and mechanical parameters of rock are shown in the tab. 1, the uniaxial compressive strength of the rock vary with temperature, as shown in [7]:

$$UCS(T) = 100\left[0.098 + \frac{0.092}{1+\left(\frac{T}{605.17}\right)^{3.2}}\right] \tag{1}$$

Effect of antenna size on the utilization of microwave energy in rock mass

Energy absorbed by materials in an electromagnetic field can be expressed by electromagnetic power loss density [8, 9]:

$$P_d = 2\pi f \varepsilon_0 \varepsilon'' E^2 \tag{2}$$

where ε_0 is the permittivity of free space, ε'' – the loss factor of the material, f – the microwave frequency in hertz, and E – the electric field strength. The electromagnetic power loss density directly determines the heating rate of rock mass, therefore, the variations in the electromagnetic power loss density of the rock mass under the influence of antenna width and height were investigated separately. As shown in fig. 2(a), the electromagnetic power loss density of the rock

mass decreases rapidly with the increase in antenna width. When the port width is 100 mm, the maximum electromagnetic power loss density is 43.95 MW/m³. If the port width increases to 300 mm, the maximum-electromagnetic-power-loss-density drops to 3.67 MW/m³. Meanwhile, the total energy absorbed by the rock mass per unit of time rises from 7265.5-8800.8 W. If the port width exceeds 300 mm, the additional increases in port size result in relatively small changes to both electromagnetic power loss density of the rock mass and the total microwave energy absorption. In addition the pronounced effect of the antenna port width on the utilization of microwave energy in rock mass, the depth of the horn antenna also has some effects on this process. As shown in fig. 2(b), the total energy absorbed by the rock mass per unit time exhibits a periodic fluctuation with the increase in antenna depth. The maximum fluctuation amplitude reaches 778.5 W. However, with increasing antenna depth, both the energy peak and the amplitude of fluctuations progressively decrease. The maximum electromagnetic power loss density fluctuates with changes in antenna depth also, but no clear pattern emerges.

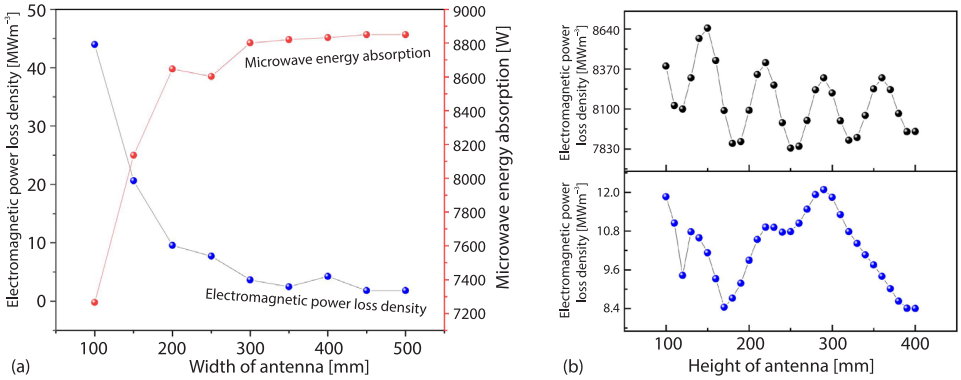

Figure 2. Electromagnetic energy absorption of rock mass under the influence of antenna size; (a) effect of antenna port width and (b) effect of antenna height

Effect of antenna size on the heating characteristics of rock mass

To further investigate the heating behavior and temperature distribution of rock mass under open-ended microwave treatment, three antenna configurations were selected, each with a height of 150 mm and port widths of 100 mm, 200 mm, and 300 mm, and the rock masses corresponding to these three configurations are denoted as L-10, L-20, and L-30. To facilitate the description of the high temperature distribution within the rock mass, the region with temperature exceeding 400 °C is designated as the effective microwave action range, while the area with temperatures above 200 °C is referred to as the microwave action range. The varying density of microwave energy on the rock surface, influenced by different antenna sizes, result in significant differences in the heating rates. Specifically, under the treatment open-ended microwave with an output power of 9 KW, the heating rates of rock samples L-10, L-20, and L-30 are 1.89 °C per ssecond, 0.56 °C per second, and 0.35 °C per second, respectively.

After 30 minutes of microwave treatment, the surface temperature of the L-10 rock mass has exceeded 1000 °C, while the surface temperatures of the L-20 and L-30 rock masses are 1004.2 °C and 636.5 °C, respectively. The remarkable thing is that along the microwave

propagation direction, the rate of temperature reduction in the L-10 rock mass is markedly higher than that observed in the L-20 and L-30 rock masses. If the depth exceeds 305 mm, the internal temperature of the L-10 rock mass falls below that of the L-20 rock mass. Figures 3(b) and 3(c) illustrates the differential distribution characteristics of the high temperature zone in the rock mass under the influence of antenna size. It can be observed that the area of the microwave action region on the rock mass surface is approximately proportional to the antenna port width. As the port width increases, the microwave action area on the surface of rock mass expands from 0.026 m² under a 100 mm port width to 0.56 m² under a 300 mm port width. In contrast, the effective microwave action region on the rock mass surface firstly increase then decrease as the antenna size increase, which is consistent with the trend of variation in the high temperature zone within the rock mass.

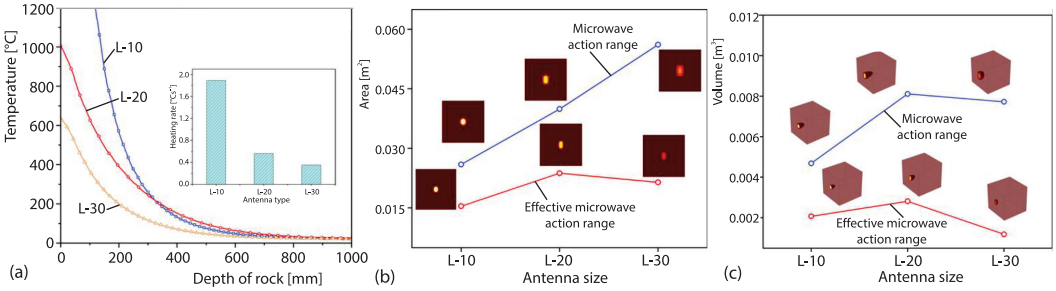

Figure 3. Heating characteristics of rock mass under the influence of antenna size;
(a) heating rates of rock masses,
(b) high temperature region distribution on the surface of rock mass, and
(c) high temperature region distribution in the interior of the rock mass

Damage evolution process of rock mass under open-ended microwave treatment

Under microwave treatment, the damage of rock mass is essentially thermal damage. Specifically, diagenetic minerals undergo uneven expansion at high temperatures, which results in a reduction in the rock's mechanical strength [10]. Additionally, the thermal gradient between the high and low temperature regions of the rock mass generates internal stress differentials, thereby promoting the initiation of macroscopic fractures. This study calculates the distribution of thermal stress within the rock mass under microwave irradiation using an electromagnetic-thermal-mechanical coupled model. And the rock damage state is then determined based on the maximum tensile stress criterion and the Mohr-Coulomb criterion, as shown in [11, 12]:

$$F_1 = \sigma_1 - f_t \quad F_2 = -\sigma_3 + \sigma_1 \frac{1+\sin\varphi}{1-\sin\varphi} - f_c \tag{3}$$

where σ_1 and σ_3 are the maximum and minimum principal stresses, φ – the internal friction angle, f_t and f_c – the tensile strength and uniaxial compressive strength of rock. When $F_1 > 0$, it is considered that the rock undergoes tensile damage. When $F_2 > 0$, it is considered that the rock experiences shear damage. After determining the failure modes in different regions of the rock mass, the degree of rock damage is further assessed using a damage variable [13, 14], *i.e.*:

$$D=\begin{cases} 0 & F_1<0,\ F_2<0 \\ \begin{cases} 0 & \varepsilon_t>\bar{\varepsilon} \\ 1-\dfrac{\lambda\varepsilon_t}{\bar{\varepsilon}} & \varepsilon_t<\bar{\varepsilon} \end{cases} & F_1\geq 0 \\ \begin{cases} 0 & \varepsilon_c<\bar{\varepsilon} \\ 1-\dfrac{\lambda\varepsilon_c}{\bar{\varepsilon}} & \varepsilon_c>\bar{\varepsilon} \end{cases} & F_1<0,\ F_2\geq 0 \\ \varepsilon_t=\dfrac{f_t}{E_0} \quad \varepsilon_c=\dfrac{f_c}{E_0} & \bar{\varepsilon}=\sqrt{(\varepsilon_1^2+\varepsilon_2^2+\varepsilon_3^2)} \end{cases} \tag{4}$$

where ε_1, ε_2, and ε_3 are the principal strain, ε_t and ε_c – the threshold strain for tensile damage and compress damage, and λ – the ratio between residual strength and initial strength of rock. The evolution of rock mass damage under microwave treatment is illustrated in fig. 4, due to the different heating rates of rock masses, L-10 rock mass is damaged after 100 seconds of 9 kW microwave treatment, while L20 and L30 rock mass are damaged after 400 seconds and 800 seconds of microwave treatment, respectively. After microwave treatment, the temperature of the rock mass in the range of the antenna port is significantly higher than that in other regions. At this stage, the high temperature zone at the center of the rock mass experiences compressive stress, while the surrounding low temperature regions are subjected to tensile stress. Given the relatively low tensile strength of the rock mass, the damage initiates in the tensile zone at the interface between the high and low temperature regions.

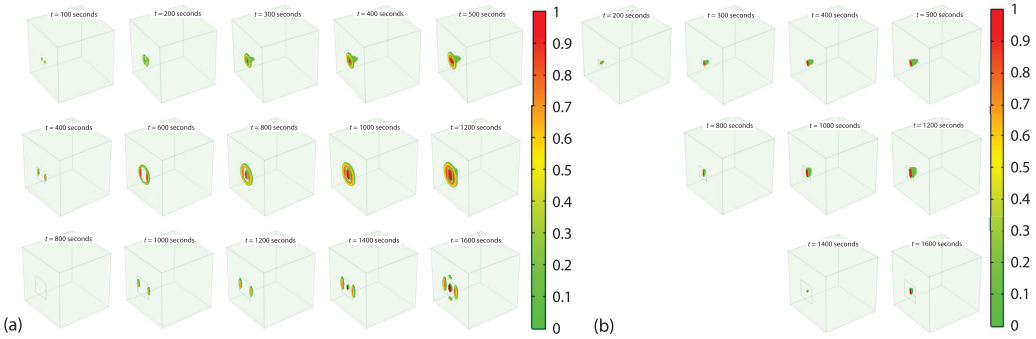

Figure 4. Rock mass damage evolution under microwave treatment; (a) no confining pressure condition and (b) confining pressure 10 MPa

As the duration of microwave treatment increases, the thermal stress in the rock mass continues to rise, leading to an expansion of the tensile damage zone and the formation of internal damage within the rock mass. Furthermore, it is observed that in the L-10 and L-20 rock masses, the damage is primarily concentrated at the surface. However, in the L-10 rock mass, the damage zone progressively extends into the interior as the microwave treatment time increases. When the confining pressure is 10 MPa, the internal stress distribution characteristics of the rock mass subjected to microwave treatment exhibit a notable shift, with the absence of a tensile stress zone within the rock mass. As a result, the onset of damage is delayed, and the damage is confined to the high temperature region within the interior of the rock mass. Consequently, the extent of the damage area is significantly reduced.

Conclusion

The size of the antenna port has a significant impact on the electromagnetic power loss density. As the antenna port size increases, the electromagnetic power loss density decreases rapidly, while the utilization of microwave energy within the rock mass improves. In addition, the influence of antenna height on microwave rock breaking effect cannot be ignored. Reducing the antenna port size can significantly enhance the efficiency of rock breaking. However, appropriately increasing the antenna size has the potential to broaden the damage zone within the rock mass. Under the treatment of a large-sized antenna, the damage to the rock mass is predominantly concentrated on the surface. In contrast, when a smaller antenna is used, the damage zone extends along the direction of microwave propagation, penetrating deeper into the interior of the rock mass.

Acknowledgment

This work was financially supported by Sichuan Science and Technology Program (2023NSFSC0004) and National Natural Science Foundation of China (52225403; 42407249; U2013603)

Nomenclature

E – electric field strength, [kVm^{-1}]
f – microwave frequency in hertz, [Hz]
f_c – uniaxial compressive strength, [MPa]
f_t – tensile strength of rock, [MPa]
T – temperature, [K]

Greek symbols

ε_c – threshold strain for compress damage, [–]
ε_t – threshold strain for tensile damage, [–]
ε_0 – permittivity of free space, [–]
ε_1, ε_2, ε_3 – principal strain, [–]
ε'' – loss factor of the material, [–]
$\bar{\varepsilon}$ – quivalent principal strain, [–]
λ – residual strength coefficient, [–]
σ_1, σ_3 – principal stress, [MPa]
φ – internal friction angle, [rad]

References

[1] Yang, B. G., *et al*., Analysis of the Thermal Mechanism and Temporal and Spatial Evolution of the Thermal Field of Deep Sandstone under Microwaves, *Thermal Science*, *24* (2020), 6B, pp. 3877-3886
[2] Wang, Y. L., *et al*., Microwave Assistance Effect for Rock Breaking of TBM Disc Cutter Using the Coupled Method of Continuum and Grain-Based Model, *Engineering Analysis with Boundary Elements*, *159* (2024), Feb., pp. 466-484
[3] Bai, Y. B., *et al*., Micro-Mechanical Properties of Main Rock-Forming Minerals in Granite under Microwave Irradiation, *Rock Mechanics and Rock Engineerin*g, *57* (2024), July, pp. 9371-9407
[4] Feng, X. T., *et a*l., An Open-end High-Power Microwave-Induced Fracturing System for Hard Rock, *Journal of Rock Mechanics and Geotechnical Engineering*, *15* (2023), 12, pp. 3163-72
[5] Ma, Z. J., *et al*., Enhancing Rock Breakage Efficiency by Microwave Fracturing: A study on Antenna Selection, *Energy*, *288* (2024), ID129876
[6] Gao, M. Z., *et al*., The Mechanism of Microwave Rock Breaking and Its Potential Application Rock-Breaking Technology in Drilling, *Petroleum Science*, *19* (2022), 3, pp. 1110-1124
[7] Gautam, P. K., *et al*., Effect of High Temperature on Physical and Mechanical Properties of Jalore Granite, *Journal of Applied Geophysics*, *159* (2018), Dec., pp. 460-474
[8] Lu, G. M., *et al*., The Influence of Microwave Irradiation on Thermal Properties of Main Rock-Forming Minerals, *Applied Thermal Engineering*, *112* (2017), Feb., pp. 1523-1532
[9] Yang, B. G., *et al*., Exploration of Weakening Mechanism of Uniaxial Compressive Strength of Deep Sandstone under Microwave Irradiation, *Journal of Central South University*, *29* (2022), 2, pp. 611-623
[10] Liu, J. J., *et al*., Experimental and Simulation Studies on Damage Characteristics, Crack Development Patterns, and Strength Reduction Mechanisms of Sandstone under Laser Irradiation, *Geomechanics and Geophysics for Geo-Energy and Geo-Eesources*, *10* (2024), 1, pp. 1-33
[11] Zhu, W. C., *et a*l., Coupled Thermal-Hydraulic-Mechanical Model During Rock Damage and Its Preliminary Application, *Rock and Soil Mechanics*, *30* (2009), 12, pp. 3851-3857

[12] Lin, H., *et al.*, Numerical Investigation of Temperature Distribution and Thermal Damage of Heterogeneous Coal under Liquid Nitrogen Freezing, *Energy*, *267* (2023), ID126592
[13] Zhu, W. C., *et al.*, Micromechanical Model for Simulating the Fracture Process of Rock, *Rock Mechanics and Rock Engineering*, *37* (2004), Nov., pp. 25-56
[14] Wei, C. H., *et al*., Numerical Simulation of Excavation Damaged Zone under Coupled Thermal-Mechanical Conditions with Varying Mechanical Parameters, *International Journal of Rock Mechanics and Mining Sciences*, *75* (2015), Apr., pp. 169-181

Paper submitted: August 20, 2024
Paper revised: November 8, 2024
Paper accepted: November 22, 2024